

# Monolithically Integrated Laser Diode and Electroabsorption Modulator with Dual-Waveguide Spot-Size Converter Output \*

Hou Lianping, Wang Wei, Feng Wen, Zhu Hongliang, Zhou Fan,  
Wang Lufeng, and Bian Jing

(National Research Center for Optoelectronic Technology, Institute of Semiconductors,  
Chinese Academy of Sciences, Beijing 100083, China)

**Abstract:** A 1.60 $\mu\text{m}$  laser diode and electroabsorption modulator monolithically integrated with a novel dual-waveguide spot-size converter output for low-loss coupling to a cleaved single-mode optical fiber are demonstrated. The devices emit in a single transverse and quasi single longitudinal mode with an SMSR of 25.6dB. These devices exhibit a 3dB modulation bandwidth of 15.0GHz, and modulator DC extinction ratios of 16.2dB. The output beam divergence angles of the spot-size converter in the horizontal and vertical directions are as small as 7.3° $\times$ 18.0°, respectively, resulting in a 3.0dB coupling loss with a cleaved single-mode optical fiber.

**Key words:** laser diode; electroabsorption modulator; spot-size converter; integrated optoelectronics; optical coupling

**EEACC:** 4320J

**CLC number:** TN248.4

**Document code:** A

**Article ID:** 0253-4177(2005)06-1094-06

## 1 Introduction

In recent years, an electroabsorption modulator (EAM) which operates using the quantum-confined Stark effect (QCSE) is attractive as an external modulator because of its many features, such as low power consumption, low drive voltage, small size, large modulation bandwidth, polarization-insensitivity, and potential for monolithic integration with other components<sup>[1-3]</sup>. An optical device integrated with a spot-size converter (SSC) has also been paid more attention for its direct coupling to an optical fiber with low-loss coupling, large align-

ment tolerances, and simple packaging schemes without using a micro-lens or tapered fiber<sup>[4]</sup>. Monolithic integration of a laser diode (or semiconductor optical amplifier) and the EAM with a SSC output (LD-EAM-SSC) is much more attractive for a transmitter module in the optical fiber communication system. This is because of its low-cost packaging due to its large spot size which is well matched to that of a single-mode fiber (SMF)<sup>[5-9]</sup>. However, most of them are based on buried structure with or without selective area growth (SAG)<sup>[3,5,6]</sup>. Moreover, most of them involve complex growth steps, excessive processing steps, strict process tolerance, and poor device performance. In

\* Project supported by the National Natural Science Foundation of China (No. 90101023), the State Key Development Program for Basic Research of China (No. 20000683-1)

Hou Lianping male, was born in 1969, PhD candidate. His research interest is in InP based photonic integrated circuits, especially in the monolithic integration of SOA, EA, and spot-size converter.

Wang Wei male, was born in 1937, professor, academician of the Chinese Academy of Sciences. His research is in InP based long wavelength semiconductor photonic devices.

Received 23 December 2004, revised manuscript received 1 March 2005

©2005 Chinese Institute of Electronics

this paper, a 1.60  $\mu\text{m}$  novel LD-EAM-SSC is fabricated by selective area growth and dual-core technology. For the LD-EAM section, a double ridge structure is employed. A ridge structure also exhibits very low capacitances, which enables, for example, high bit-rate operation in integrated laser-modulators<sup>[10]</sup>. For the SSC section, a buried ridge double-core structure (BRS) is incorporated. The combination of the ridge and BRS structure can take advantage of both the easy processing of the ridge structure and the excellent mode characteristic of the BRS. This is the first time that such a structure is reported, as far as we know. Furthermore, the novel LD-EAM-SSC was easily fabricated using only three steps low-pressure metal-organic vapor phase epitaxial (LP-MOVPE) growth and a conventional photolithography and wet etching process. More important, the device emits in a single transverse mode and quasi single longitudinal mode with a side mode suppression ratio (SMSR) of 25.6 dB, although no grating is fabricated in the LD region. Furthermore, these devices exhibit a 3 dB modulation bandwidth of 15.0 GHz, and modulator DC extinction ratios of 16.2 dB. The output beam divergence angles of the spot-size converter in the horizontal and vertical directions are as small as  $7.3^\circ \times 18.0^\circ$ , respectively, resulting in a 3.0 dB coupling loss with a cleaved single-mode optical fiber. All the performance indexes are as good as or better than those of other counterparts<sup>[3,5,6]</sup>.

## 2 Device structure and fabrication

Figure 1 shows the schematic structure of the LD-EAM-SSC. The output end of the device has a 300  $\mu\text{m}$ -long dual-waveguide SSC, for which the active core is linearly tapered from 3  $\mu\text{m}$  to 0  $\mu\text{m}$  along with the propagation direction while its passive core is 8  $\mu\text{m}$ -wide and 50 nm-thick, a 0.2  $\mu\text{m}$  InP spacer layer between them. So in the LD and EAM section most optical power is confined in the active core. However, in the SSC section, the optical power is gradually transferred to the passive core along

with the SSC active core becoming narrow. Eventually, at the output facet of SSC, the optical mode is determined only by the thin passive core, which is designed to expand and stabilize the beam from the LD and EAM for efficient coupling to an SMF. Followed the SSC regions are the LD and EAM sections. The LD and EAM sections are 600  $\mu\text{m}$ -long and 150  $\mu\text{m}$ -long, respectively, with a 50  $\mu\text{m}$ -long etched electrical isolation region between them. A conventional double ridge waveguide structure is used for the LD and EAM region. However, a buried ridge double-core structure (BRS) is incorporated for the SSC regions.

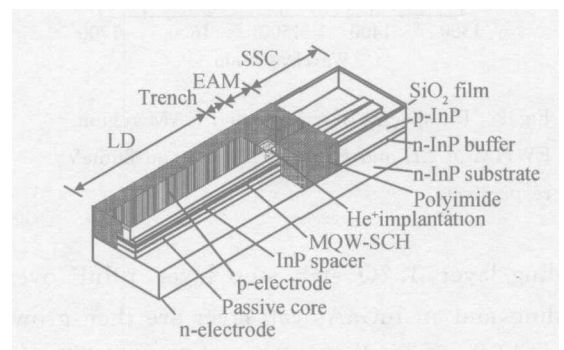


Fig. 1 Schematic diagram of the LD-EAM-SSC

The LD-EAM-SSC is fabricated using a only three-step LP-MOVPE process, one of which is the SAG step. For the first epitaxial growth, InP buffer, 50 nm-thick n-type 1.15  $\mu\text{m}$  bandgap InGaAsP quaternary (Q) lower waveguide and a 0.2  $\mu\text{m}$  n-InP spacer layer are grown. Then, two SiO<sub>2</sub> pads are patterned on the spacer layer in the LD region. The MQW-SCH stack is then grown. The MQW structure consists of ten strained InGaAsP quantum wells and nine InGaAsP barriers, SCH layers (100 nm,  $\lambda = 1.2 \mu\text{m}$ ) on both sides of the MQW-layer. The oxide pads cause an enhancement of the growth rate and a reduction of the bandgap energy of the Q-waveguide in the middle of the gap between the oxide pads. The SAG process creates a bandgap difference between the modulator and the laser diode of 75 nm as measured with small-spot photoluminescence (see Fig. 2). After removing the SiO<sub>2</sub>, the lateral taper is formed by selective etch-

ant of MQW-SCH layers from the SSC regions. A sharp taper tip less than  $0.4\mu\text{m}$  at the SSC section is easily achieved by normal photolithography combined with an undercut etching. So, there is no need for a submicron patterning using expensive and time-consuming e-beam lithography. A thin p-InP

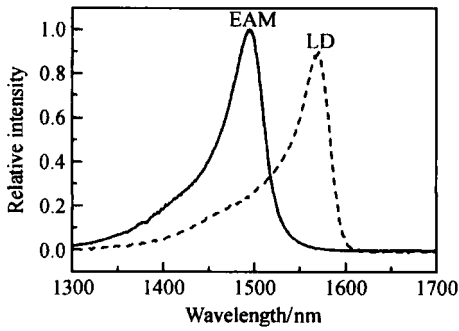


Fig. 2 PL spectra of the LD and EAM region  
FWHM of LD and EAM is  $27\text{meV}$  and  $26\text{meV}$ , respectively.

cladding layer,  $1.2\mu\text{m}$  etch stop layer, p-InP overcladding, and an InGaAs cap layer are then grown in the third epitaxial growth step. This is followed by conventional double ridge waveguide processing of the LD and EAM sections. The width of the LD and EAM upper mesa and the maximum width of the lower mesa are  $3\mu\text{m}$  and  $8\mu\text{m}$ , respectively (see Fig. 3). The LD and EAM are electrically isolated by etching away the highly conductive InGaAs cap layers between the two sections and  $\text{He}^+$  is implanted in the trench. Figure 1 illustrates these described features. To eliminate the excess light ab-



Fig. 3 SEM picture of EAM transverse section

sorption in the InGaAs cap layer (lattice matched InGaAs has an absorption wavelength of  $1.67\mu\text{m}$ ) in the SSC regions, the InGaAs cap layer in the SSC region is entirely etched away. A  $\text{SiO}_2$  dielectric layer is then deposited on the wafer. Polyimide is defined on either side of the LD and EAM mesa for planarization of its ridge structure and reduction of EAM spurious capacitance of the p contact pads to enhance the modulation bandwidth. After a contact hole is etched on the top of the LD and EAM ridges, standard p- and n-metal layers are evaporated.

### 3 Device performance

The typical lasing wavelength of the LD-EAM-SSC is around  $1.60\mu\text{m}$  at  $25^\circ\text{C}$  and the breakdown voltage of the EAM is at  $-10\text{V}$ . Isolation electric resistance between the LD and EAM section is more than  $100\text{k}\Omega$  while the total EAM capacitance is  $0.4\text{pF}$  at a reverse bias of  $2\text{V}$  which leads to a  $3\text{dB}$  modulation bandwidth of  $15.0\text{GHz}$ .

Figure 4 shows the laser typical optical spectrum of the device at  $198\text{mA}$  and  $25^\circ\text{C}$  when the EAM biased voltage is  $0\text{V}$ . Quasi single longitudinal mode is observed with an SMSR of  $25.6\text{dB}$ , although no grating is fabricated in the LD region. This is probably because the interfaces among the LD, EAM, and SSC divide the whole cavity length into some sub-sections, and the optical frequencies that are resonant with any of the sub-section lengths are enhanced. The mode selection is caused

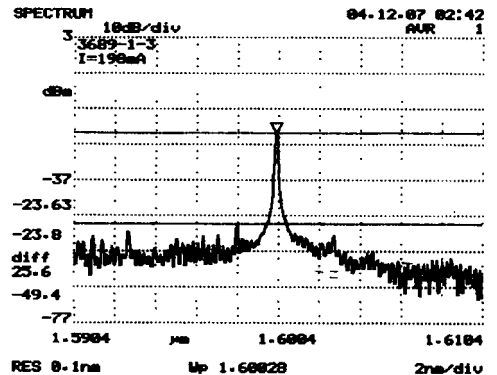


Fig. 4 Emission spectrum of the LD-EAM-SSC

by refraction of the mode on the scale of the cavity rather than by diffraction at the scale of the emission wavelength.

Figure 5 shows the function of SMSR versus the LD drive current. As the current is increased, the SMSR is increased to 25.7 dB at 180 mA. Further increase in the current causes the SMSR to decrease. At the same time, the lasing wavelength of the LD-EAM-SSC is almost around 1.60 μm as long as the temperature is kept at 25 °C.

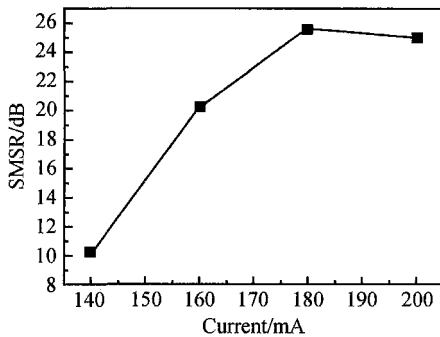


Fig. 5 SMSR versus LD drive current

Figure 6 shows the *P-I* characteristics of the device when the modulator is biased. There is no significant degradation of the threshold and the output light power observed in the integrated devices with a different length of SSC the region in the same wafer, which indicates that there is no large excess absorption loss at the introduction of the SSC. As can be seen in this figure, as the reverse bias voltage increases, the threshold current of the device increases monotonically. This threshold current increment is due to the electroabsorption induced by the reverse bias on the modulator. Note the abrupt turning on of the *P-I* characteristics which is a common feature of this kind of devices. From these *P-I* characteristics, one can see that when the bias voltage on the modulator is varied from 0 to -2.5 V while the current injection on the laser is fixed at 160 mA, the on-off ratio is larger than 16.2 : 1, normally on operation.

Figure 7 shows the far field pattern observed from the SSC facet and that from the rear facet of the LD (In Fig. 7(b), there is a side lobe at an an-

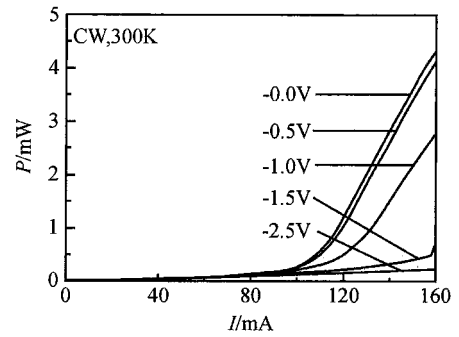


Fig. 6 *P-I* characteristics of the device when the modulator is biased

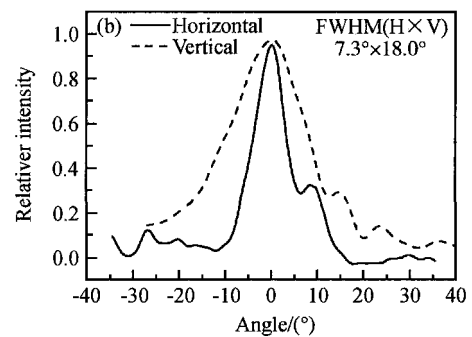
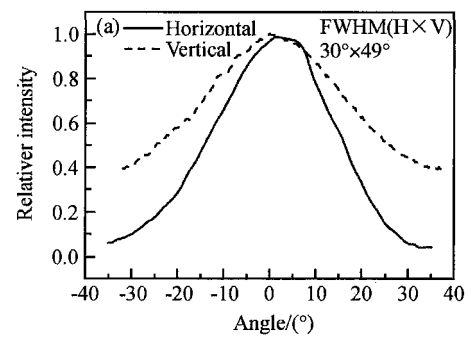


Fig. 7 Far-field pattern from the laser rear facet (a) and SSC facet (b)

gle of 10 ° in a horizontal FFP, which is caused by the reflected light from the submount). As can be seen in this figure, the LD-EAM-SSC emits in a single transverse mode, which indicates that there is no degradation of single transverse mode characteristics at the introduction of the SSC. The divergence angles from the SSC facet are as small as 7.3 ° × 18.0 ° in the horizontal and vertical directions, respectively. In contrary, those from the rear facet of the LD are as large as 30.0 ° and 49 °. The coupling loss and 1 dB align tolerance for the SSC

facet are about 3.0dB,  $\pm 3.1\mu\text{m}$  (horizontal)  $\times$   $\pm 2.65\mu\text{m}$  (vertical), when the device is coupled to a cleaved SMF. However, at the same case, those from the rear facet of the LD are about 9dB,  $\pm 2.0\mu\text{m}$  (horizontal)  $\times$   $\pm 1.7\mu\text{m}$  (vertical).

## 4 Conclusion

A 1.60 $\mu\text{m}$  laser diode and electroabsorption modulator monolithically integrated with a novel dual-core spot-size converter output for low-loss coupling to a cleaved single-mode optical fiber is demonstrated. The devices emit in a single transverse and quasi single longitudinal mode with an SMSR of 25.6dB. The DC extinction ratio of 16.2dB is observed for the device with a modulator bias of 2.5V. The output beam divergence angles of the spot-size are as small as  $7.3^\circ \times 18.0^\circ$ , in the horizontal and vertical directions, respectively, resulting in low-coupling losses with a cleaved optical fiber (3.0dB loss). Simple fabrication procedure and excellent performance make the device suitable for mass-production and a cost-effective active, or passive, mode locked laser<sup>[11,12]</sup>. If both side of mirrors are AR coated, the device will become the structure of SOA-EAM-SSC, which offers a single compact device incorporating both signal amplifier and modulation functions as well as spot-size conversion.

## References

- [ 1 ] Devaux F, Dorgeuille F, Ougazzaden A, et al. 20Gbit/s operation of high-efficiency InGaAsP/InGaAsP MQW electroabsorption modulator with 1.2-V drive voltage. *IEEE Photonics Technol Lett*, 1993, 5(11):1288
- [ 2 ] Ido T, Sato H, Moss DJ, et al. Strained InGaAs/InAlAs MQW electro-absorption modulators with large bandwidth and low driving voltage. *IEEE Photonics Technol Lett*, 1994, 6(10):1207
- [ 3 ] Devaux F, Bordes P, Ougazzaden A, et al. Experimental optimization of MQW electroabsorption modulators with up to 40GHz bandwidths. *Electron Lett*, 1994, 30(16):1347
- [ 4 ] Lestra A, Emery J Y. Monolithic integration of spot-size converters with 1.3- $\mu\text{m}$  lasers and 1.55- $\mu\text{m}$  polarization insensitive semiconductor optical amplifiers. *IEEE J Sel Topics Quantum Electron*, 1997, 3(6):1429
- [ 5 ] Koren U, Miller B I, Young M G, et al. Polarization insensitive semiconductor optical amplifier with integrated electroabsorption modulators. *Electron Lett*, 1996, 32(2):111
- [ 6 ] Johnson J E, Ketelsen L J P, Grenko J A. Monolithically integrated semiconductor optical amplifier and electroabsorption modulator with dual-waveguide spot-size converter input. *IEEE J Sel Topics Quantum Electron*, 2000, 6(1):19
- [ 7 ] Choi W J, Bond A E, Kim J. Low insertion loss and low dispersion penalty InGaAsP quantum-well high-speed electroabsorption modulator for 40-Gb/s very-short-reach, long-reach, and long-haul applications. *J Lightwave Technol*, 2002, 20(12):2052
- [ 8 ] Beck M, Abdallah O, Charles W L. 40-Gb/s tandem electroabsorption modulator. *IEEE Photonics Technol Lett*, 2002, 14(1):27
- [ 9 ] Asaka K, Suzuki Y, Kawaguchi Y. Lossless electroabsorption modulator monolithically integrated with a semiconductor optical amplifier and a passive waveguide. *IEEE Photonics Technol Lett*, 2003, 15(5):679
- [ 10 ] Lesterlin D, Artigaud S, Rodrigues V. High performance and reproducible integrated laser modulator for 10Gb/s NRZ transmission over standard fiber. *Proc ECOC*, 1996, 3:289
- [ 11 ] Sato K, Wakita K, Kotaka I, et al. Monolithic strained-InGaAsP multiple-quantum-well lasers with integrated electroabsorption modulators for active mode locking. *Appl Phys Lett*, 1994, 65(1):1
- [ 12 ] Arahira S, Oshiba S, Matsui Y, et al. 500GHz optical short pulse generation from a monolithic passively mode-locked distributed Bragg reflector laser diode. *Appl Phys Lett*, 1994, 64(15):1917

## 半导体激光器电吸收调制器和双波导模斑转换器的单片集成\*

侯廉平 王 圩 冯 文 朱洪亮 周 帆 王鲁峰 边 静

(中国科学院半导体研究所 光电子研究发展中心, 北京 100083)

**摘要:** 报道了 1.6 $\mu\text{m}$  的半导体激光器和电吸收调制器以及双波导模斑转换器的单片集成器件. 该器件具有良好的单横模特性和准单纵模特性(边模抑制比达 25.6dB), 3dB 调制带宽为 15GHz, 直流消光比为 16.2dB, 远场发散角为  $7.3^\circ \times 18.0^\circ$  和单模光纤的耦合效率达 3.0dB.

**关键词:** 半导体激光器; 电吸收调制器; 模斑转换器; 光电子集成; 光耦合

**EEACC:** 4320J

**中图分类号:** TN248.4

**文献标识码:** A

**文章编号:** 0253-4177(2005)06-1094-06

\*国家自然科学基金(批准号:90101023), 国家重点基础研究发展计划(批准号:20000683-1)资助项目

侯廉平 男, 1969 年出生, 博士研究生, 主要从事 InP 基 SOA, EA 及 SSC 的单片集成.

王 圩 男, 1937 年出生, 教授, 中国科学院院士, 主要研究 InP 基长波长半导体光电子器件.

2004-12-23 收到, 2005-03-01 定稿